The chemical fixation of carbon dioxide to propylene carbonate over triazabicyclodecene-functionalized silica nano catalyst

Muazu Samaila Batagarawa and Farook Adam
Department of Pure and Industrial Chemistry, Umaru Musa Yaradua UniversityPMB 2218, Katsina Nigeria
School of Chemical Sciences, Universiti Sains Malaysia, 11800 Penang, Malaysia

Abstract.

Silica from Rice husk ash (RHA) was extracted and functionalized with 1, 5, 7-triazabicyclo [4.4.0] dec-5-ene (TBD) guanidine. The functionalized silica-guanidine material was used as a catalyst for the synthesis of cyclic carbonates from the reaction of CO2 with different epoxides. The catalyst was prepared, first by the reaction of 3-(chloropropyl)triethoxy silane (CPTES) with silica at room temperature and pressure to form chloro propyl silica material (RHACCl). It was later grafted with TBD guanidine at refluxing temperature of 110 °C to form the solid catalyst (RHAPrTBD). Among the characterizations employed to prove the successful incorporation of the guanidine onto silica, the solid state NMR for 13C showed the presence of all the carbon atoms on the structure. Both XRD and TEM results also proved the amorphous nature of the catalyst. Under the optimized reaction conditions, the CO2 was reacted with other epoxides to give the corresponding five-membered cyclic carbonates in good yield. The catalyst was recovered and reused few more times. However, some decrease in the conversion was observed during the recycle process. This might be attributed to loss of the catalyst during the re-cycle process. Based on the result obtained a proposed mechanism was also suggested.

Keywords: triazabicyclodecene, silica-guanidine, nanoparticles, carbon dioxide, propylene oxide, propylene carbonate.

1.0 Introduction.

Guanidine is nitrogen based organic compound widely used in the synthesis of heterocyclic compounds. It is found in the side-chain of the amino acid, arginine and plays an important role in the interaction with enzymes or receptors through hydrogen bonding and/or electrostatic interactions, because of its strong basic character [1]. Guanidine has been used both as a homogeneous and heterogeneous catalysts in several base catalyzed organic reactions, such as Michael addition [2], [3], transesterification of vegetable oils [4], methylation of phenol [5], aldol and knoevenagel condensation reactions [6], esterification of glycerol [7] and in cyclo addition of carbon dioxide to cyclic carbonate [8], [9], [10], [11], [12] [13]. Several homogeneous guanidine and related imine compounds have been reported as catalysts in the conversion of CO_2 and epoxides to cyclic carbonates. But these catalysts have drawbacks such as, separation from reaction mixture, need for co-solvents, low activity/selectivity, corrosion problems and non-recyclability.

Takahashi et al. [12], reported the application of immobilized synergistic hybrid catalysts such as phosphonium salts for the conversion of CO_2 and epoxides to cyclic carbonates. Results show a remarkable acceleration in the conversion of propylene oxide to propylene carbonate, due to the synergistic participation of both the onium and silanol group from the silica source. However, low yield was obtained, when the salt

was supported on a polymer based compound.

Similarly, the use of bio polymer products such as chitosan for the functionalisation of ammonium salt was shown to be active in the synthesis of propylene carbonate from Propylene oxide [13]. The catalyst was reported to be recyclable and easy to regenerate.

However, biopolymers can degrade with time and therefore render the catalyst in-effective. The design of a suitable catalyst to activate CO_2 into more useful products must take cognizance of energy input, eco-friendly process and simple work-up procedure. In this context therefore, the use of supercritical carbon dioxide, or the application of higher temperature during catalyst preparations are obvious limitations.

The conversion of carbon dioxide into useful products has dual significances in view of both environmental protection and sustainable chemistry [13]. One of the most promising methodologies in this area is the synthesis of cyclic carbonates via the cyclo addition of epoxides and CO_2. While the utilisation of CO_2 will reduce its level in the atmosphere, at the same time, its cyclo addition with other compounds will open an opportunity for its conversion to useful products. This promotes green chemistry and sustainable development [14].

Cyclic carbonates have several applications notably, as polar aprotic solvents, as precursors in the production of polycarbonate materials and as intermediate in organic synthesis. The synthesis of cyclic carbonates, by the reaction of CO_2 with cyclic ethers could be an alternative to avoid the use of the highly toxic phosgene compounds.

We recently reported the heterogenisation of linear guanidine molecule (1,1,3,3-tetramethylguanidine), on the silica support and investigated its catalytic activity on the reaction of CO_2 with propylene oxide, to form propylene carbonate in good yield [11]. In this work, bicyclic guanidine was used for the same reaction but without using any solvent.

2. 0 Materials and methods.

2.1 Reagents and chemicals

All chemicals and solvents used were of AR grade and purchased commercially and used without further purification. The chemicals used in this study includes: (3-chloroprophyl) triethoxysilane (CPTES) (Merk ≥ 95 %), tetramethylguanidine (Sigma Aldrich 99 %), nitric acid (Systerm 65 %), and sodium hydroxide (QRec 99 %). Triethylamine (Sigma Aldrich 99 %). Propylene oxide (ACROS 99 %). Acetonitrile (QREC 99.5%). Dichloromethane (QRec 99.5 %). Toluene, unhydrous (Sigma Aldrich 99.8%), Acetone (QReC 99 %) and acetophenone (Sigma Aldrich 99 %). The rice husk was collected from a rice mill in Penang, Malaysia.

2.2 Preparation of Rice Husk Ash (RHA)

Rice husk ash (RHA) was prepared according to a reported method [15]. The husk was obtained from a rice mill in Penang, Malaysia. It was washed with water, discarding the suspended husk, rinsed with distilled water and dried at room temperature for 24 h. The cleaned RH (100 g) 700 mL 1.0 M

nitric acid at room temperature for 24 h, and washed with distilled water until constant pH. It was subsequently dried in an oven at 100 °C for 24 h, and calcined at 600 °C for 6 h for complete combustion. The white rice husk ash obtained was ground to fine powder, and labeled as RHA.

2.3 Grafting of (3-chloropropyl)triethoxysilane on the silica by sol-gel method.

The preparation of silica supported chloropropyl triethoxysilane was according to a reported method [16]. 3.00 g of the RHA was suspended in 100 mL of 0.6 M NaOH in a plastic container and stirred for 1 h at 80 °C resulting in complete dissolution. The solution was filtered to remove undissolved particles. A 6.00 mL solution of (3-chloropropyl) triethoxysilane (CPTES) was added to the sodium silicate solution, and titrated slowly with 3.0 M nitric acid with constant stirring. The change in pH was monitored by using a pH meter. A white gel started to form when the pH approached 10. The titration was stopped at pH ~ 3. The gel obtained was aged for 48 hours in a covered plastic container at 80 °C. It was centrifuged at 4000 rpm for 8 min (Rotina 38, Hittich Zentrifugn) for separation. The process of washing and separation was repeated 6 more times with copious amount of distilled water and finally with dichloromethane. The sample was dried at room temperature for 1 h, then at 110 °C for 24 h. It was ground to fine powder, and labeled as RHACCl.

2.4 Preparation of RHAPrTBD

The post synthetic grafting technique was used for the functionalization of the silica with1,5,7-triazabicyclo[4.4.0]dec-5-ene (TBD). In the synthesis, 3.5 mL (27.89 mmol) of 1,5,7-triazabicyclo[4.4.0]dec-5-ene was added to a suspension of RHACCl (1.0 g) in anhydrous toluene (30 mL) and triethylamine 3.9 mL (27.89 mmol) as deprotonating agent. The reaction mixture was refluxed at 110 °C in an oil bath for 24 h. The solid product was filtered off, washed with sufficient amount of toluene, and dried at 100 °C for 24 h to afford RHAPrTBD catalyst. Scheme 1 shows the equation of the synthesis.

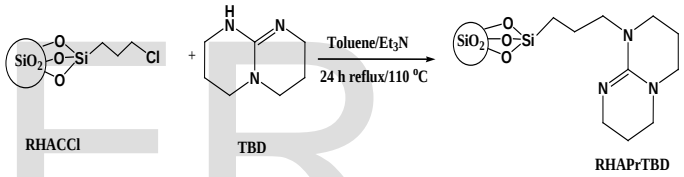

Scheme 1. The synthesis of RHAPrTBD from RHACCl and TBD.

2.5 Characterization

Elemental analysis was performed with a Perkin Elmer Series II, 2400 micro elemental analyzer. The infrared spectrum was obtained in the 400-4000 cm^{-1} range, using Perkin-Elmer 2000 FT-IR spectrometer. Thermo gravimetric analysis (TGA) was carried out on TGA/DTA SDTA 851^e analyzer at a heating rate of 20 °C min^{-1}. X-ray powder diffraction (XRD) patterns were recorded using Cu Kα radiation source, on a Siemens Diffractometer, D5000, Kristalloflex. Nitrogen physisorption measurements were conducted using a Micromeritics Autosorb-1 CLP, Quantachrom, USA. Samples were pretreated

by heating under vacuum at 120 °C for 10 h. The surface area was analyzed by the BET method, and the pore size distribution was determined using the BJH method applied to the adsorption branch of the isotherm. Transmission electron microscopy (TEM) studies were performed using Philips CM 12 instrument (Eindhoven, Netherlands), equipped with Docu version 3.2 image processing software (Munster, Germany). The solid samples were suspended in absolute ethanol. One droplet of the suspension was placed on a carbon film coated with 400 mesh copper grid and allowed to stand for 1-3 min.

The solid state ^{29}Si and ^{13}C CP/MAS NMR experiments were performed on a Bruker AVANCE, 400 MHz Spectrometer, equipped with a magic angle-spinning (MAS). The sample was spun at 8.0 kHz in a 4.0 mm outer diameter zirconia ceramic rotor spinner. The proton decoupling was applied. The ^{13}C chemical shifts were referenced to TMS using solid adamantine as a secondary standard.

The scanning electron microscopy (SEM) studies were carried out using Leo Supra 50 VP Field Emission Scanning Electron Microscope, equipped with Oxford INCA 400, energy dispersive X-ray microanalysis (Carl-Zeiss SMT, Germany). Before the analysis, the powdered sample was mounted on an SEM specimen stub consisted of double–sided sticky tape. Gas chromatographic (GC) analyses were performed using GC (Clarus 500 Perkin Elmer) equipped with a flame ionization detector (FID) and a capillary wax column (length = 30 m, inner diameter = 0.25 mm and film thickness = 0.25 μm). The GCMS was carried out using a Clarus 600 (Perkin Elmer) under similar conditions.

2.6 Catalytic activity

The cycloaddition reaction of CO_2 with propylene oxide was carried out in a 100 mL autoclave (PVT Amar Equipments, India) equipped with a magnetic stirrer, in which was placed appropriate amount of the catalyst, and propylene oxide. The specified amount of CO_2 was charged into the autoclave and was heated to the desired temperature. The reaction was carried out for 1 – 10 h. At the end of the reaction, the reactor was allowed to cool to room temperature. The excess pressure was vented off. The catalyst was removed by centrifuge. The reaction products were monitored by gas chromatography. Acetophenone was used as internal standard. The products were further confirmed with GC-MS.

3.0 Results and discussion

3.1 The N_2 adsorption desorption and elemental analysis

Fig.1 shows the N_2 adsorption isotherms of RHAPrTBD. The functionalized sample displayed type IV isotherm with type H2 hysteresis loop associated with capillary condensation in its mesopores. Since type IV isotherm is associated with mesoporous material, this indicated that, the catalyst was mesoporous even after the functionalisation with the TBD. However, the BET surface area and pore volume decreased after the functionalisation, possibly due to the presence of –$(CH_2)_3$TBD groups within the pore (Table 1). The pore size also decreased from 4.45 nm in RHACCl to 3.60 nm. The

catalyst had a narrow uniform pore size distribution as can be seen inset. Narrow pore size distribution is indications of excellent textural uniformity of material [9] and can contribute to high selectivity of products.

Table 1
Summary of N_2 adsorption-desorption and elemental analyses for RHAPrTBD. The C, H and N content were determined by a combination of elemental and EDX analysis (average values).

	Elemental analysis (%)						Pore diam. (nm)
	C	H	N	Si	S_{BET} (m^2g^{-1})	Pore vol. (ccg^{-1})	
RHACCl	8.35	2.30	-	(24.39)	625	0.26	4.43
RHAPrTBD	23.11	4.75	7.56	-	326	0.16	3.60
	(37.42)	-	(17.71)	(9.25)			

The values in parenthesis were obtained by EDX elemental analysis

3.2. The Fourier Transform Infrared Spectroscopy analysis (FT-IR)

The FT IR spectra of RHAPrTBD is shown in Fig.2. The large and broad bands between 3442 and 3413 cm^{-1} in both RHACCl and RHAPrTBD are associated with O-H stretching frequency of silanol groups and the adsorbed water. The bands at 2950 cm^{-1} in both RHACCl and RHAPrTBD are due to C-H stretching vibrations. The Si–O–Si stretching vibrations at 1092 cm^{-1} for RHACCl, was shifted to 1068 cm^{-1} in RHAPrTBD.

The absorption band 1639 cm^{-1} in RHAPrTBD is due to the combined effect of the angular vibration of water molecules and the C=N stretching vibration [17], [18]. Only the angular vibration of water molecules can be seen for the RHACCl at 1645cm^{-1} which was much less intense. Similarly, the vibration at 1530 cm^{-1} is ascribed to antisymmetric stretching vibration of C-N bond, which is in good agreement with the data reported elsewhere [18].

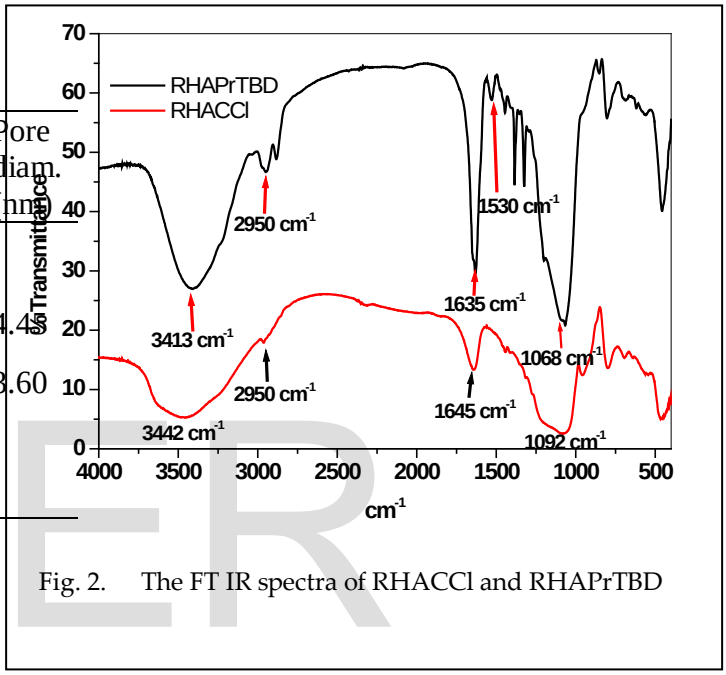

Fig. 2. The FT IR spectra of RHACCl and RHAPrTBD

3.3. The ^{13}C CP/MAS NMR spectroscopy of RHAPrTBD

Figure 3 shows the ^{13}C CP/MAS NMR spectra of RHAPrTBD. Eight chemical shifts in the range of 0.60-151 can be seen for RHAPrTBD. The first two chemical shifts at δ = 0.6, 9.7 ppm were assigned to C1 and C2 atoms of the propyl chain attached to the silica network. The characteristic peaks, viz; C3, C4 (δ = 21 ppm); C5 (δ = 47 ppm); C6, C7 (δ = 38 ppm); C8 (δ = 26 ppm) were also observed. The effect of lone pair on the Nitrogen atom, shifted the signal of C9 to appear slightly down field (δ =64 ppm). The last carbon atom, labeled as C10,

appeared at down field, this was due to the presence of pi electrons on the C=N bond, which caused the carbon atom to be deshielded and therefore appeared at down field position (δ = 151 ppm) [19]. The presence of these peaks further confirmed the immobilisation of the guanidine molecule on the silica.

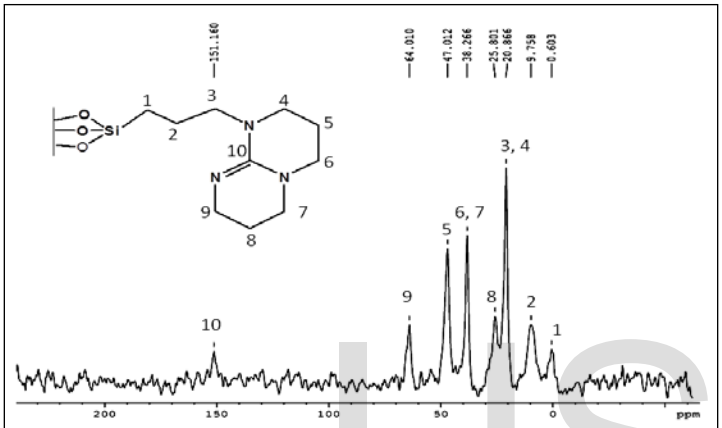

Fig. 3. The solid state ^{13}C CP/MAS NMR for RHAPrTBD showing the chemical shift for the various carbon atoms present in the structure.

3.4. The ^{15}N MAS NMR spectroscopy of RHAPrTBD catalyst

The ^{15}N spectra for the catalyst RHAPrTBD showed two chemical shifts at 78 and 84 ppm (Fig.4). The presence of these two peaks could be attributed to the resonance structures which exist in separate but closely related chemical environments for the silica immobilized catalyst.

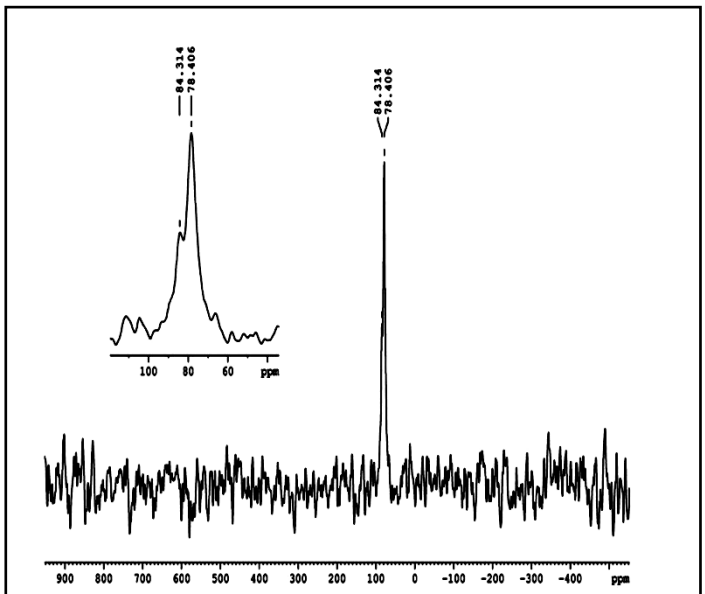

Fig. 4. The solid state ^{15}N NMR spectra of RHAPrTBD, showing a sharp and intense peak at 78 ppm and a shoulder peak at 84 ppm chemical shifts. Inset is the expanded form of the two peaks.

3.5. The Thermo gravimetric / differential thermal analyses (TGA/DTA)

10 mg of the catalyst, RHAPrTBD was used to study its thermal behaviour using differential thermal analysis (DTA) (Fig. 5). The TGA of the catalyst showed three characteristic decomposition stages: the first, starting from 29–139 °C with a maximum at 54 °C, was due to loss of adsorbed water (ca. 5.44 %); the second mass loss (ca. 16.47 %, 1.66 mg) occurred between 139 and 411°C with a maximum at 275 °C, was due to the decomposition of TBD molecule on the silica surface. Using this mass loss, it was calculated that 1.20 mmol g^{-1} of RHAPrTBD was loaded on the silica support [20]. The third continuous mass loss (ca.12.05 %) occurred between 400 and 750 °C with a maximum at ca. 650 °C, this was attributed to

the dehydration of entrapped water molecules deep within the silica frame work and the loss of water due to formation of siloxane bonds by the condensation of neighboring silanol groups [21]. The TGA–DTA provided further evidence for the successful immobilisation of TBD on RHACCl to form RHAPrTBD.

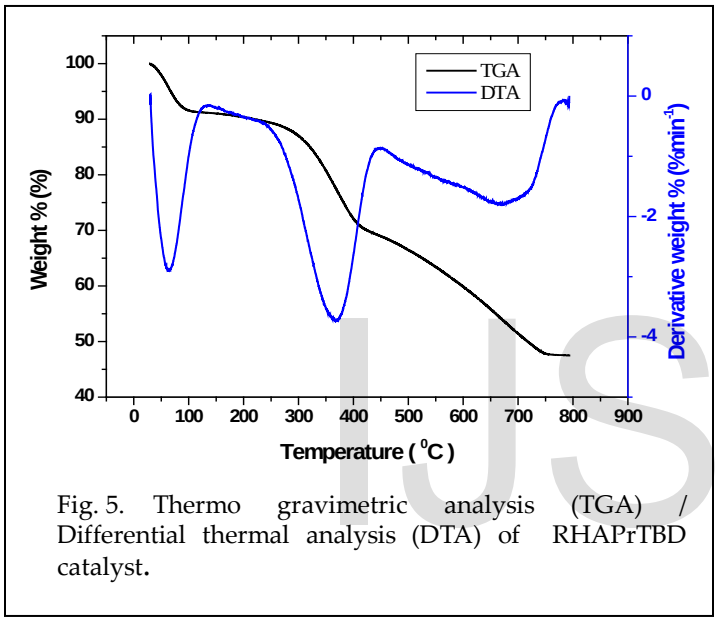

Fig. 5. Thermo gravimetric analysis (TGA) / Differential thermal analysis (DTA) of RHAPrTBD catalyst.

3.6. The Transmission Electron Microscopy (TEM)

The transmission electron micrographs (TEM) at various magnifications for the RHAPrTBD are shown in Fig. 6. The high degree of homogeneity of RHAPrTBD shows that the sample is granular and porous. The granular particles have almost spherical shape with a particle range of 20-30 nm. These results corroborates well with the N-sorption data since both indicate relatively small average pore size.

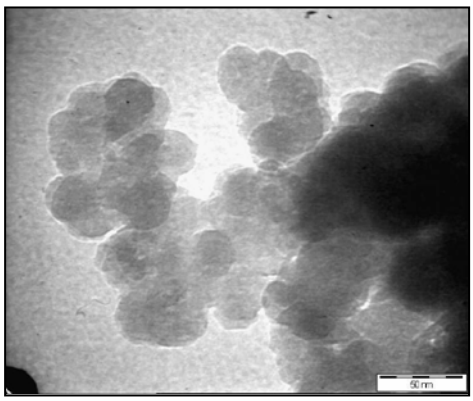

Fig.6.Transmission Electron Microscopy of RHAPrTBD, showing some spherical nano particle structures. The scale bar corresponds to 50 nm.

3.7. The effect of reaction parameters on the cyclo addition of CO_2 to propylene oxide under solvent-less condition

The cyclo addition reaction of CO_2 with propylene oxide was carried out in a high pressure reactor using RHAPrTBD as the catalyst. No solvent was used in the reaction. The reaction was carried out at 50 bar CO_2 pressure at 130 °C for 10 h. Equation 1 shows the synthesis of Propylene Carbonate (PC) from Propylene Oxide (PO). A control test run without the catalyst, but with rice husk silica was found to be inactive for the reaction under the same reaction conditions.

3.7.1 The effect of time on the conversion of PO to PC over RHAPrTBD

The dependence of propylene oxide conversion on the reaction time was investigated by using 0.2 g of RHAPrTBD at 120 °C. As expected, longer reaction times resulted in higher conversions due to the prolonged contact between the reactants and the catalyst. Figure 7 shows the time

dependence on the conversion of propylene oxide over RHAPrTBD. The conversion of propylene oxide at 2h was 48.1 %, and this increased to a maximum of 92.7 % in 10 h. The selectivity of propylene carbonate was 97 % which did not change over the course of the reaction. The increased conversion of PO to PC and better selectivity are related to the catalysts high basic strength as suggested by Zhang et al [9].

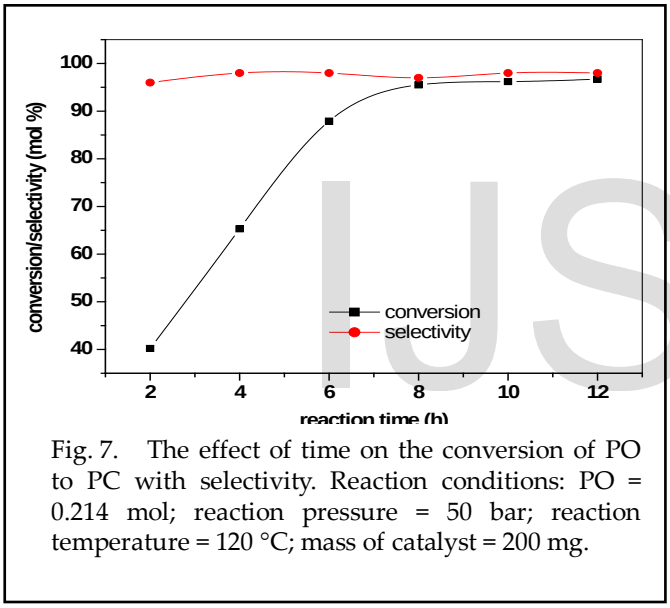

Fig. 7. The effect of time on the conversion of PO to PC with selectivity. Reaction conditions: PO = 0.214 mol; reaction pressure = 50 bar; reaction temperature = 120 °C; mass of catalyst = 200 mg.

3.7.2 The effect of reaction temperature

The results in fig. 8 show that the reaction temperature has a strong effect on propylene oxide conversion. In the catalytic reactions conducted at temperature from 100 to 140 °C, the propylene oxide conversion obtained was in the range of 68.4 to 95.1 % respectively. The high conversion-rate was attributed to higher reactivity at higher temperatures [14].

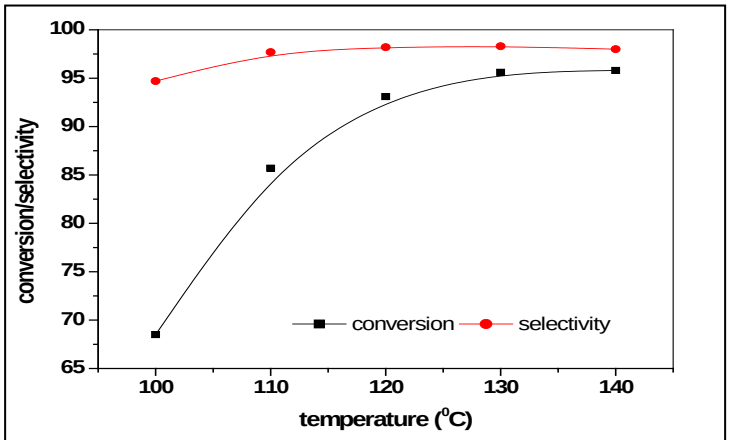

Fig. 8. The effect of temperature on the conversion of PO to PC with selectivity. Reaction conditions: PO = 0.214 mol; reaction pressure = 50 bar; reaction time = 10

.

3.7.3 The effect of carbon dioxide pressure

The influence of CO_2 pressure on the conversion of PO is shown on Fig. 8. When the CO_2 pressure was increased progressively from 20 to 50 bar, the propylene oxide conversion also increased from 57.6 % to 92.5 % respectively. At higher pressure (60 bar) the propylene oxide conversion did not change significantly. Wang et al. [14] suggested that high CO_2 pressure could cause low concentration of PO around the vicinity of the catalyst, which may result in low PC yield. A CO_2 pressure of 50 bar was the optimum pressure for the reaction using RHAPrTBD as the catalyst

.

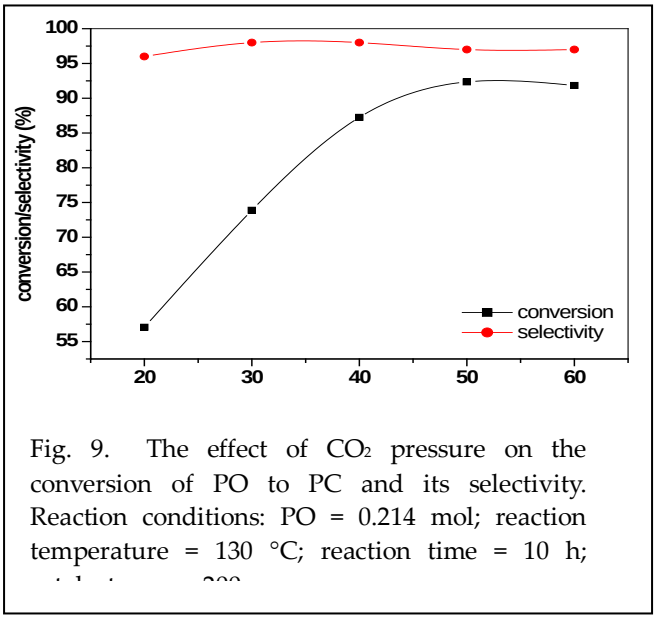

Fig. 9. The effect of CO_2 pressure on the conversion of PO to PC and its selectivity. Reaction conditions: PO = 0.214 mol; reaction temperature = 130 °C; reaction time = 10 h;

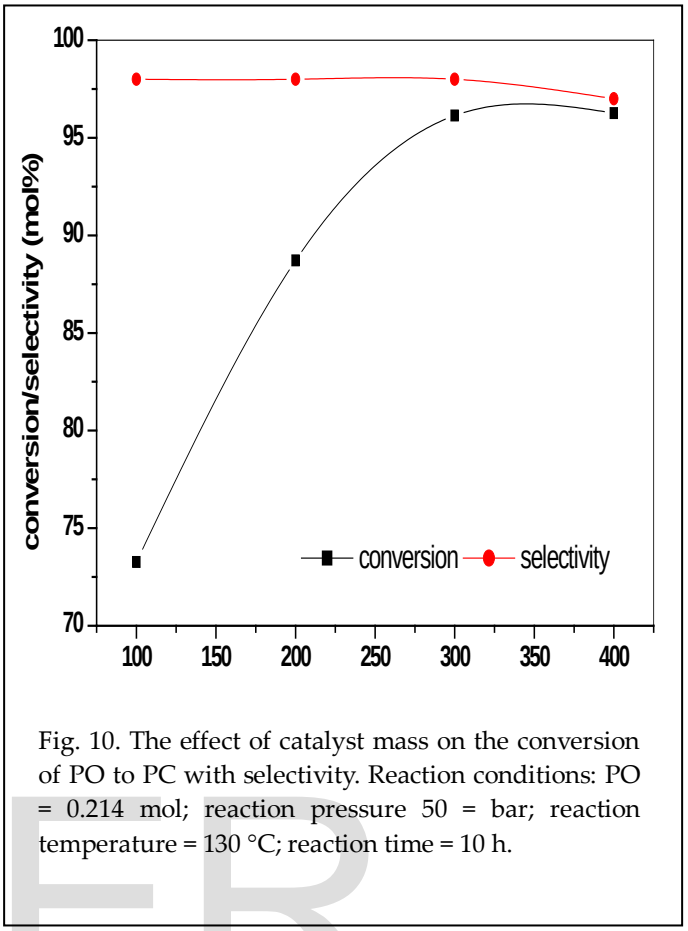

Fig. 10. The effect of catalyst mass on the conversion of PO to PC with selectivity. Reaction conditions: PO = 0.214 mol; reaction pressure 50 = bar; reaction temperature = 130 °C; reaction time = 10 h.

3.7.4 The effect of catalyst mass

The effect of catalyst loading was examined by using 100, 200, 300 and 400 mg catalyst mass. As shown in Fig. 10, the conversion of PO increased as the catalyst mass was increased from 100 mg to 300 mg, attaining a maximum conversion of 96.1 %. Further increase in the mass of catalyst did not yield any significant change in the conversion. Thus, 300 mg was found to be the optimum mass of catalyst for the reaction. The variation in mass of the catalyst has no significant influence on the selectivity, and the major product obtained was propylene carbonate.

3.7.5 Reusability test

A series of catalytic cycles were run to investigate the stability of RHAPrTBD. In each case, the catalyst was recovered by separating it from the reaction mixture by centrifuge. It was then followed by rinsing with acetone, dried at 110 °C for 3 h and reused for subsequent reaction. In each cycle, the reaction was performed under the optimized conditions. The conversion of PO and the selectivity in the subsequent runs (2^{nd} – 3^{rd} cycle) shows some decrease in the conversion, which could be ascribed to leaching. The FT- IR spectra of the reused catalyst (Fig. 11) showed the presence of sharp peaks at 1567 and 1461 cm^{-1} which are due to –C=NH-

and –C-NH vibrations from the guanidine molecule [17]. Similarly, the broad absorption band at 1733 cm^{-1} also shows the presence of C=O stretching vibration from the chemically adsorbed CO_2 molecule [22]. This indicated that, direct contact between CO_2 and the catalyst occurred on the active site.

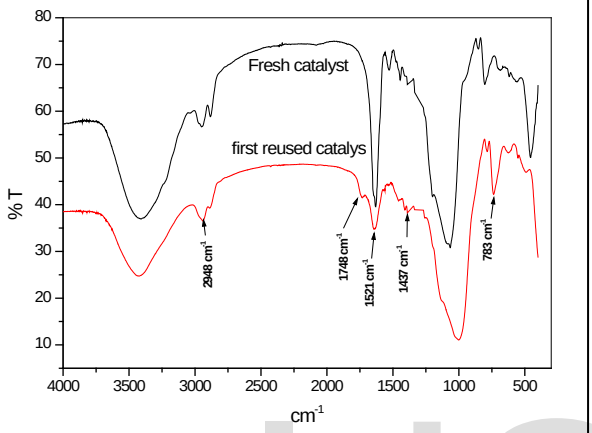

Fig. 11. The FT IR of the fresh and reused catalyst, showing the presence of absorption band at 1748 cm^{-1} which was associated with C=O stretching from CO_2 molecule.

3.7.6 Proposed reaction mechanism

A possible reaction mechanism for the cyclo addition of CO_2 to epoxides over RHAPrTBD is shown in Scheme 3. The activation of CO_2 by guanidine has been reported previously [22]. Our latest investigation shows positive interaction between homogeneous guanidine and carbon dioxide even at ambient conditions. The CO_2 is thought to be adsorbed on the surface of the Lewis base sites (-N=) to form carbamate specie. The guanidinium cation formed is stabilized by resonance which leads to lowering of energy in the overall system. Similarly, the carbonate anion attacks the less sterically hindered carbon atom of the epoxide to which opens the epoxide ring. The resulting anion attacks the carbonyl carbon intra-molecularly, forming the five membered ring propylene carbonate which leaves the catalytic surface, thereby regenerating the catalyst.

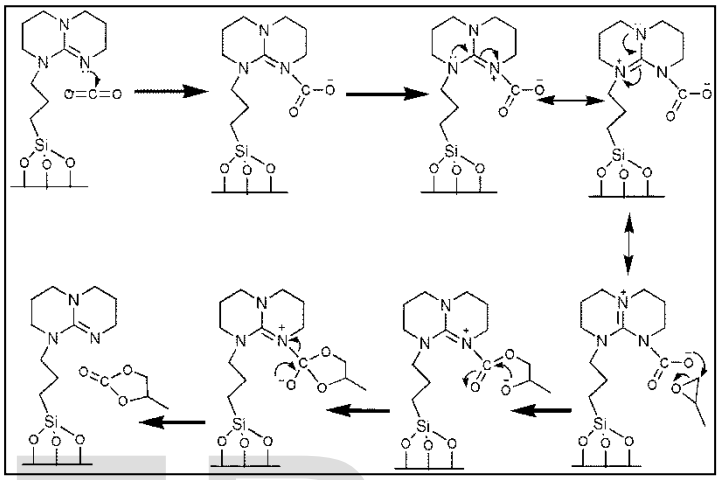

Scheme 3. The proposed reaction mechanism showing the fixation of CO_2 by the N= basic site from the guanidine. The resonance structure of the guanidinium cation stabilised the energy of the system. Subsequent attack of the epoxide by the carbonate anion opens the ring. Intramolecular rearrangements of the system lead to the formation of five member cyclic carbonate, with restoration of the catalyst.

4. Conclusion

Heterogeneous guanidine catalyst based on 1,5,7-triazabicyclo[4.4.0]dec-5-ene guanidine was prepared by functionalisation via chloroprophyl group, previously attached to an amorphous silica. The work up procedure for the synthesis of the catalysts was quite easy, and eco-friendly, without the use of toxic chemicals.

Characterisation of the catalysts proved that indeed the intended organic groups were successfully immobilised onto the silica surface. The catalyst was found to be active and highly selective towards the synthesis of propylene carbonate from the reaction of CO_2 with propylene oxide without the use of any solvent.

The catalyst was also found to be recycleable and reusable, for at least three times. The little decrease in catalytic activity observed was attributed to leaching of the active component, probably due to continuous heating. The reaction time, temperature, pressure and amount of catalyst was found to have significant effect on the reaction. The catalyst was recovered and subjected to three further cycles.

5 Acknowledgment

The authors are grateful to Education Trust Fund (ETF), Umaru Musa Ya'adua University Katsina, Nigeria for the scholarship to M.S.B. and Universiti Sains Malaysia for the RU grant 101/ PKIMIA/8440 which in part, supported this research.

References

1. L. R. de Assuncao, E. R. Marinho, & F. P. Proenca, *ARKIVOC* (v) (2010) 82-91.
2. W. Ye, J. Xu, C. -T. Tan & C.-H. Tan, *Tetrahedron Lett., 46 (2005) 6875-6878.*
3. D. Ma, & K. Cheng, *Tetrahedron: Asymmetry, 10 (1999) 713–719.*
4. R. Sercheli, R. M. Vargas & U. Schucchardt, *J. Am. Oil Chem. Soc.76, 10 (1999) 1207-1210.*
5. G. Barcelo, D. Grenoillat, J. P. Senet, & G. Sennyey, *Tetrahedron 46, 6 (1990) 1839-18.*
6. T. Takahashi, T. Watahiki, S. Kitazume, H. Yasuda, & T. Sakakura, *Chem. Commun.*(2006) *1664-1666.*
7. R. Sercheli. A. L.B. Ferreira, M. C. Guerreiro, R. M. Vargas, R. A. Sheldon & U. Schuchardt, *Tetrahedron Lett., 38, 8, (1997) 1325-1328.*
8. F. Jerome, G. Kharchafi., I. Adam & J. Barrault, *Green Chem., 6 (2004) 7 2 – 7 4.*
9. X. Zhang, N. Zhao, W. Wei, & Y. Sun, *Catal. Today, 115 (2006) 102-106.*
10. A. Barbarini., R. Maggi, A. Mazzacani. G. Mori, G. Sartori. & R. Sartorio, *Tetrahedron Lett., 44 (2003) 2931–2934.*
11. Adam, F., & Batagarawa, M. S. *Appl. Catal. A: General. (2012) 164-171.*
12. T. Takahashi, T. Watahiki, S. Kitazume, H. Yasuda & T. Sakakura, *Chem. Commun.* (2006) *1664-1666.*
13. Y. Zhao, J. S. Tian. X. H. Qi., Z. N. Han, Y.Y. Zhuang & L. N. He, *J. Mol. Catal., A Chem., 271 (2007) 284-289.*
14. J. Q. Wang, X. D. Yue, F. Cai & L. N. He, *Catal. Commun. 8 (2007) 167-172*
15. A. E. Ahmed & F. Adam, *Micropor. Mesopor. Mater. 103 (2007) 284-295*.
16. F. Adam, K. M. Hello & H. Osman, *J. Colloid Interf. Sci. 331 (2009) 143–147.*
17. A. C. Blanc, D. J. Macquarrie, S. Valle, G. Renard, C. R. Quinnb & D. Brunel, *Green Chem., 2 (2000) 283–288.*
18. E. A. Faria, H. F. Ramalho, J. S. Marques, P. A. Z. Suarez & A. G. S. Prado, *Appl. Catal. A 338 (2008) 72-78.*
19. P., Kalita & Kumar, R. Kumar , *Appl. Catal. A, 397* (2011), 250-258.
20. F. Adam, K.M. Hello & H. Osman, *Appl. Catal. A* 382 (2010) 115–121.
21. F. Adam, K.M. Hello, & T.H. Ali, *Appl. Catal. A* 399 (2011) 42–49.

22. F. S., Pereira, E. R., de Azevedo, E. F., da Silva, T. J., Bonagamba, D. L., da Silva Agostíni, A. Magalhães, & E. R., Pérez González, (2008). *Tetrahedron*, *64*(43), 10097-10106.